JOURNAL OF CHEMICAL & ENGINEERING DATA

ARTICLE

pubs.acs.org/jced

Thermodynamic Properties of Plant Biomass Components. Heat Capacity, Combustion Energy, and Gasification Equilibria of Cellulose

Andrey V. Blokhin, Olga V. Voitkevich, Gennady J. Kabo,* Yauheni U. Paulechka, Margarita V. Shishonok, Andrey G. Kabo, and Vladimir V. Simirsky

Chemistry Faculty and Research Institute for Physical Chemical Problems, Belarusian State University, Leningradskaya 14, 220030 Minsk, Belarus

Supporting Information

ABSTRACT: Heat capacities and enthalpies of formation were determined for the well-characterized samples of cellulose of different origins. The obtained experimental results allowed us to obtain the accurate values of thermodynamic properties for this material. It was demonstrated that the heat capacity and entropy of cellulose samples can be linearly related with their crystallinity index. The equilibria of the processes of cellulose gasification were considered. The adiabatic temperatures of the gasification and energetic characteristics of the products of cellulose thermolysis were evaluated.

INTRODUCTION

The use of plant biomass as fuel and raw material for chemical processing is being increased.[1] The effective operation of energy and processing plants using plant biomass is possible if their working conditions are thermodynamically justified. However, very limited information about thermodynamic properties of cellulose and lignin, the major components of the stem part of biomass, is available. In refs 2 to 3 the heat capacity of cellulose fibers was measured in a drop calorimeter. The heat capacity changes near T = 400 K corresponding to the glass transition were observed. Hatakeyama et al.[4] measured heat capacity of cellulose in the temperature range of (330 to 450) K by differential scanning calorimetry (DSC) and found no anomalies below T = 440 K. In refs 5 to 8 the heat capacity of cellulose was determined in adiabatic calorimeters. Karachevtsev and Kozlov[6] measured the heat capacity in a range of temperatures of (80 to 300) K for two samples dried by different methods and found that the results depend on the method of drying. Uryash et al.[8] determined the heat capacity for cotton microcrystalline cellulose in the temperature range (80 to 330) K. In ref 8 the anomalies at 291 K, 343 K, and 403.5 K were observed in the differential thermal analysis (DTA) curve, and the first anomaly was also found in the heat capacity curve. The energies of combustion for various samples of cellulose were also reported in ref 8 though the samples were not characterized by the ash content.

In this work the heat capacities in the temperature range of (5 to 370) K and the enthalpies of formation were determined for the samples of cellulose of different origins and degrees of crystallinity. The obtained experimental results allowed us to obtain the reliable values of thermodynamic properties of cellulose required for the calculation of equilibria of the reactions with the participation of this compound, the adiabatic temperatures of the processes of its gasification, and energetic characteristics of the products of cellulose thermolysis.

EXPERIMENTAL SECTION

Preparation and Characterization of Samples. Four cellulose samples of different structures from various sources were used in this study: (1) cotton microcrystalline cellulose "Ankir";[9] (2) wood sulfite cellulose from Koryazhma Branch of Ilim Group (Kotlas Pulp and Paper Mill) prepared according to TU-5411-027-05711131-95 standard; (3) straw cellulose obtained by nitric acid delignification of rape straw stems according to ref 10; and (4) wood amorphous cellulose obtained by regeneration of cellulose from the nitrogen(IV) oxide−ethyl acetate solution according to the procedure described in ref 11.

Prior to the measurements, all of the samples were dried at 403 K for (40 to 60) h until the constant mass was reached. This treatment was then followed by keeping the samples over P_2O_5 at room temperature for at least 72 h. The ash content in the samples was determined from the mass of residue after combustion in a calorimetric bomb. The sulfur content was determined by a gravimetric method with the use of the saturated barium chloride solution.[12] It was assumed that sulfur in the samples was contained in the form of sulfate salts. Since this is the most oxidized form of sulfur, there was no need to introduce the appropriate correction to the combustion energy. At least three experiments were made for each determination. The results are presented in Table 1.

The degree of crystallinity of the cellulose samples was determined from X-diffractograms with a HZG-4a diffractometer (Cu Kα radiation source, Ni filter). The measurements were performed in a step mode. The cellulose samples were prepared in the form of flat discs of equal mass using the press-out technique. Since the X-ray data indicated that the crystalline part of samples 1 to 3 was the crystal of cellulose I (see below), the

Received: March 17, 2011
Accepted: July 2, 2011
Published: July 28, 2011

Table 1. Index of Crystallinity and Mass Fractions of Ash and Sulfur in the Studied Samples of Cellulose

sample	I_c	$w(\text{ash})/\%$	$w(\text{S})/\%$
1	0.90	0.10 ± 0.01	0.02 ± 0.01
2	0.80	0.10 ± 0.01	0.43 ± 0.01
3	0.74	0.49 ± 0.03	0.11 ± 0.01
4		0.07 ± 0.01	0.02 ± 0.01

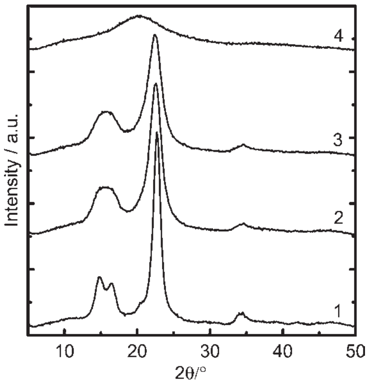

Figure 1. X-ray patterns for cellulose samples 1 to 4.

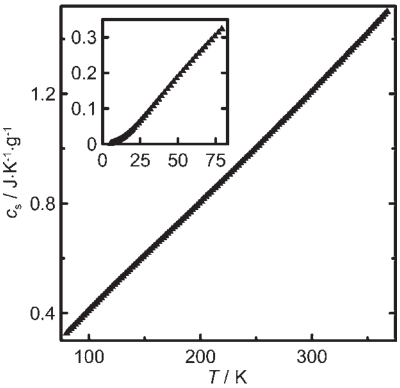

Figure 2. Experimental heat capacities c_s for microcrystalline cellulose.

crystallinity index (I_c) was calculated from the patterns recorded in the identical conditions according to Segal et al.:[13]

$$I_c = \frac{I_{002} - I_a}{I_{002}} \qquad (1)$$

where I_{002} is the maximum intensity of the (002) lattice diffraction and I_a is the intensity of diffraction corresponding to the amorphous halo near 19°. For the samples studied in this work, I_{002} was determined at $2\theta = 22.7°$, and I_a was determined at $2\theta = 18.7°$.

The heat capacity of cellulose in the temperature range of (5 to 370) K was measured in a TAU-10 adiabatic calorimeter (Termis, Moscow).[14] The detailed description of the calorimeter construction and the experimental procedures was published earlier.[15] The temperature was measured with an Fe/Rh resistance thermometer (R_0 = 50 Ω) calibrated on ITS-90 by VNIIFTRI (Moscow). The relative uncertainty of the heat capacity measurements is $\pm 4 \cdot 10^{-3}$ over the main temperature range of (20 to 370) K and does not exceed $\pm 2 \cdot 10^{-2}$ at $T < 10$ K.

Table 2. Experimental Heat Capacities for Microcrystalline Cellulose (1)

T/K	$c_s/\text{J}\cdot\text{K}^{-1}\cdot\text{g}^{-1}$
Series 1	
5.44	0.001557
5.68	0.001793
5.92	0.002074
6.18	0.002431
6.48	0.002853
6.78	0.003329
7.09	0.003799
7.41	0.004309
7.73	0.004810
8.06	0.005358
8.40	0.005933
8.73	0.006544
9.07	0.007174
9.42	0.007835
9.77	0.008513
10.12	0.009239
10.58	0.01022
11.13	0.01144
11.69	0.01274
12.26	0.01416
12.83	0.01567
13.41	0.01723
13.99	0.01893
14.58	0.02071
15.16	0.02269
15.86	0.02526
16.66	0.02821
17.47	0.03123
18.28	0.03442
19.09	0.03770
19.91	0.04109
21.03	0.04595
22.47	0.05246
23.93	0.05942
25.39	0.06644
26.86	0.07360
28.34	0.08090
30.15	0.09001
31.80	0.09824
33.61	0.1074
35.43	0.1165
37.25	0.1258
39.08	0.1350
41.02	0.1447
43.05	0.1549
45.08	0.1651
47.13	0.1754
49.18	0.1854
51.24	0.1954
53.30	0.2052
55.37	0.2151
57.45	0.2251

Table 2. Continued

T/K	c_s/J·K^{-1}·g^{-1}
59.53	0.2349
61.62	0.2448
63.71	0.2545
65.81	0.2641
67.91	0.2735
70.01	0.2830
72.22	0.2929
74.53	0.3031
76.85	0.3134
79.17	0.3235
81.50	0.3335
83.83	0.3433
Series 2	
80.07	0.3271
81.97	0.3353
83.89	0.3434
85.80	0.3512
87.72	0.3593
89.64	0.3673
91.57	0.3756
93.49	0.3838
95.42	0.3921
97.36	0.4004
99.29	0.4083
101.22	0.4163
103.16	0.4244
105.11	0.4327
107.06	0.4407
109.02	0.4485
110.97	0.4566
112.93	0.4644
114.88	0.4726
116.84	0.4806
118.80	0.4885
120.77	0.4964
122.73	0.5043
124.70	0.5118
126.68	0.5199
128.65	0.5279
130.62	0.5357
132.60	0.5437
134.58	0.5513
136.57	0.5593
138.55	0.5671
140.55	0.5748
142.54	0.5825
144.53	0.5904
146.53	0.5983
148.52	0.6061
150.52	0.6137
152.52	0.6218
154.52	0.6293
156.53	0.6370
158.53	0.6450

Table 2. Continued

T/K	c_s/J·K^{-1}·g^{-1}
160.54	0.6525
162.55	0.6604
164.56	0.6682
166.57	0.6758
168.58	0.6837
170.59	0.6914
172.61	0.6991
174.62	0.7068
176.64	0.7147
178.66	0.7223
180.67	0.7302
182.69	0.7381
184.71	0.7461
186.73	0.7539
188.75	0.7615
190.77	0.7692
192.79	0.7775
194.81	0.7853
196.83	0.7930
198.86	0.8010
200.88	0.8088
202.90	0.8171
204.93	0.8249
206.96	0.8329
208.99	0.8407
211.01	0.8486
213.04	0.8563
215.07	0.8645
217.11	0.8722
219.14	0.8803
221.17	0.8883
223.20	0.8962
225.73	0.9061
227.76	0.9140
229.80	0.9219
231.83	0.9304
233.86	0.9388
235.89	0.9469
237.92	0.9552
239.95	0.9633
241.99	0.9711
244.02	0.9790
246.05	0.9871
248.08	0.9954
250.11	1.004
252.14	1.012
254.17	1.020
256.20	1.029
258.23	1.037
260.26	1.045
262.30	1.053
264.33	1.061
266.35	1.069
268.38	1.078

Table 2. Continued

T/K	c_s/J·K^{-1}·g^{-1}
270.41	1.087
272.44	1.095
274.47	1.103
276.50	1.112
278.53	1.120
280.56	1.128
282.59	1.137
284.61	1.145
286.63	1.153
288.65	1.162
290.68	1.170
292.70	1.178
294.73	1.187
296.75	1.195
298.77	1.204
300.79	1.212
302.81	1.221
304.83	1.230
306.85	1.239
308.87	1.247
310.89	1.255
312.91	1.265
314.94	1.273
316.96	1.282
318.98	1.290
321.00	1.300
323.02	1.308
325.04	1.316
327.07	1.325
329.09	1.333
331.12	1.343
333.14	1.352
335.16	1.360
337.19	1.368
339.21	1.377
341.24	1.384
343.27	1.394
345.29	1.402
347.32	1.410
349.34	1.420
351.35	1.429
353.37	1.438
355.39	1.447
357.41	1.456
359.43	1.465
361.44	1.473
363.46	1.482
365.48	1.491
367.50	1.500

The experimental heat capacities were smoothed with the polynomial equations. For all of the polynomials, the root-mean-square (rms) deviations of experimental points from the smoothing curves did not exceed half of the uncertainty in the corresponding temperature range.

The combustion energies of the cellulose samples were determined in a combustion calorimeter equipped with a stainless-steel bomb of 326 cm^3 volume.[16] The energy equivalent of the calorimeter $\varepsilon_{\text{calor}}$ = 14595.5 ± 4.2 J·K^{-1} was determined from 10 experiments on combustion of benzoic acid (K-2 grade, mass fraction purity of 0.99993). A Pt crucible was used in the combustion experiments. The initial oxygen pressure in the bomb was 3.09 MPa. The compressed pellets for calorimetric experiments were kept over P_2O_5. When a pellet was loaded into the calorimetric bomb, its exposition to air did not exceed 10 min. The change of the pellet mass during this period was insignificant.

Differential scanning calorimetry (DSC) and thermogravimetric (TG) analyses were performed with a Netzsch STA 449 Jupiter instrument. The sample of about 4 mg mass was placed in an aluminum crucible. The curves in the temperature range (300 to 873) K were recorded at a 10 K·min^{-1} scanning rate under nitrogen gas.

■ RESULTS AND DISCUSSION

X-ray Phase Analysis. An X-ray pattern of microcrystalline cellulose (1) is characterized by clear, well-resolved, intense reflections (Figure 1, curve 1). A narrow strong maximum at 2θ = 22.7°, a resolved doublet with the maxima at 2θ = 14.9° and 16.5°, and a reflection at 2θ = 34.5° indicate a high degree of lattice perfection of cotton cellulose as well as the large size and zero defects of its crystallites. The crystallinity index of this sample was found to be 90 %.

The samples of wood (2) and straw (3) cellulose have a lower crystallinity index (curves 2 and 3 in Figure 1). A comparison of diffraction patterns 1, 2, and 3 (Figure 1) confirms a substantially lower degree of structural order of the fibrillar samples compared to the microcrystalline one that is caused by presence of the amorphous phase. The unresolved doublet at the diffraction angles (14 to 16)° and the wider maximum close to 22.7° indicate imperfection and a relatively small size of crystallites both for wood and straw fibrillar cellulose. The crystallinity index for the cellulose samples is presented in Table 1. Figure 1 demonstrates that the crystalline part of samples 1 to 3 represents the native polymorphic modification of cellulose, cellulose I, and the observed reflections correspond to the following crystallographic planes: 14.9° to (101); 16.5° to $(10\bar{1})$; 22.7° to (002); 34.5° to (040).[13]

Cellulose regenerated from solution was studied as the sample with the extreme disordering. The X-ray diffractogram pattern of the regenerated cellulose (4) is an amorphous halo with a diffused maximum at about 20° (Figure 1, curve 4).

Heat Capacity. Experimental molar heat capacities $C_{p,\text{m}}$ of sample 1 in a range of temperatures, (5 to 370) K, are presented in Figure 2. The experimental heat capacities of samples 1 (Table 2) and 2 in the temperature interval (5 to 370) K and samples 3 and 4 in the temperature interval (80 to 370) K are presented in Table S1 to S3 of Supporting Information. No phase transitions or anomalies in the heat capacity curves for all of the samples were found.

Heat capacity of samples 3 and 4 was extrapolated below T = 80 K according to Kelley et al.[17] with the use of the equation:

$$\frac{C_{p,i}(T)}{C_{p,1}(T)} = a_i + b_i T \tag{2}$$

where $C_{p,i}(T)$ is the heat capacity of the ith sample at temperature T. The a_i and b_i coefficients were found by the method of least-squares from the smoothed heat capacities in the temperature ranges (80 to 230) K for sample 3 and (80 to 160) K for sample 4. The rms deviation of the experimental values from those calculated according to eq 2 did not exceed $6 \cdot 10^{-4}$.

The relative deviations of heat capacities for samples 2, 3, and 4 from that of microcrystalline cellulose (1) are presented in Figure 3. The relative deviation of heat capacity for sample 2 reached 10 % near 15 K which is probably caused by the different content of mineral components. At the same time, this deviation did not exceed 2 % in the range of (250 to 370) K. The relative deviation for sample 3 was less than 1 % in the range of (80 to 130) K and 3.3 % near 370 K. The maximum deviation of 6.6 % for amorphous cellulose (4) was observed in the temperature range of (330 to 370) K. We analyzed the possible effect of mineral impurities on the heat capacity of cellulose above $T = 100$ K and concluded that it will not exceed the experimental uncertainty in this case.

The standard molar thermodynamic functions were calculated per the monomeric unit of cellulose based on the polynomial equations for the temperature dependence of heat capacity. The smoothed values of heat capacity and thermodynamic functions for the different samples of cellulose are presented in Table 3 and Table S4 of Supporting Information.

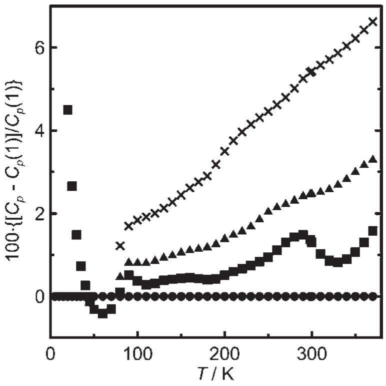

Figure 3. Relative deviation of heat capacity for samples 2, 3, and 4 from that of microcrystalline cellulose (1): ●, microcrystalline (1); ■, wood (2); ▲, straw (3); ×, amorphous (4).

As follows from the data obtained (Figure 4, Table 3, and Tables S1 to S4 of Supporting Information), the cellulose sample with the highest crystallinity index possesses the lowest heat capacity and thermal part of entropy that seems to be physically reasonable. One may assume that the heat capacity and entropy of cellulose at a given temperature T linearly changes with the crystallinity index I_c:

$$C_{p,\mathrm{m}}(T)/\mathrm{J \cdot K^{-1} \cdot mol^{-1}} = a(T) + b(T)I_c \quad (3)$$

$$\Delta S_\mathrm{m}(T)/\mathrm{J \cdot K^{-1} \cdot mol^{-1}} = d(T) + e(T)I_c \quad (4)$$

The values of the a, b, d, and e parameters at different temperatures (Table 4) were found from the smoothed heat capacities and entropies of samples 1 to 3. Relative deviations of the heat

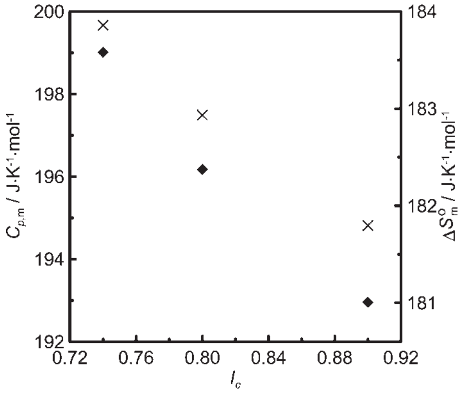

Figure 4. Heat capacity (×) and entropy (◆) of cellulose samples 1 to 3 at 298.15 K.

Table 4. Values of the *a*, *b*, *d*, and *e* Parameters from eqs 3 and 4

T/K	a	b	d	e
100	69.69	−3.387	54.41	−3.798
150	105.0	−6.513	89.32	−5.655
200	140.4	−11.07	124.3	−8.038
250	181.0	−20.48	159.8	−11.37
298.15	221.7	−29.96	195.2	−15.83
300	223.1	−30.10	196.6	−16.02

Table 3. Thermodynamic Properties for Microcrystalline Cellulose (1)

T	$C_{p,\mathrm{m}}$	$\Delta_0^T H_\mathrm{m}°/T$	$\Delta_0^T S_\mathrm{m}°$	$-(G_\mathrm{m}°(T) - H_\mathrm{m}°(0))/T$	$-\Delta_f H_\mathrm{m}°$	$-\Delta_f G_\mathrm{m}°$
K	$\mathrm{J \cdot K^{-1} \cdot mol^{-1}}$	$\mathrm{J \cdot K^{-1} \cdot mol^{-1}}$	$\mathrm{J \cdot K^{-1} \cdot mol^{-1}}$	$\mathrm{J \cdot K^{-1} \cdot mol^{-1}}$	$\mathrm{kJ \cdot mol^{-1}}$	$\mathrm{kJ \cdot mol^{-1}}$
0	0	.	0	.	943.5	943.5
50	30.70	11.98	18.30	6.312	953.4	915.7
100	66.67	30.59	50.97	20.38	963.1	873.9
150	99.18	48.10	84.23	36.13	970.0	827.8
200	130.6	64.80	117.1	52.26	975.9	779.5
273.15	178.0	88.70	164.7	76.00	983.0	706.4
298.15	194.8	96.89	181.0	84.12	985.0	681.0
300	196.1	97.50	182.2	84.72	985.1	679.1
400[a]	265	131	248	117	990	576
500[a]	329	164	314	150	991	473
580[a]	377	190	367	176	988	390

[a] Thermodynamic functions were extrapolated using eqs 5 and 6.

capacities and entropies calculated from eqs 3 and 4 did not exceed 0.5 % over the temperature range of (80 to 370) K.

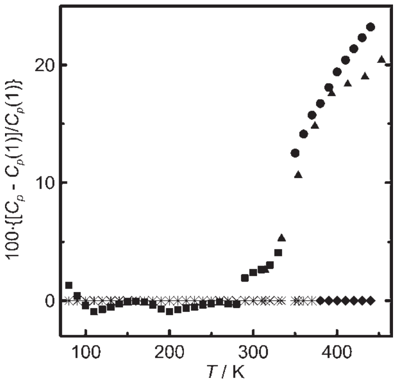

Figure 5. Comparison of experimental data on the heat capacity of cellulose: ∗, microcrystalline cellulose $[C_p(1)]$ (this work); ◆, extrapolated by eqs 5 and 6; ▲, ref 3; ●, ref 4; ■, ref 8.

Table 5. B3LYP/6-31G(d) Vibrational Wavenumbers for the Glucose Molecule

w^a/cm^{-1}
71, 108, 122, 171, 209, 221, 245, 281, 302, 339, 346, 386, 400, 409, 420, 427,
447, 479, 538, 555, 588, 619, 673, 903, 1015, 1029, 1043, 1052, 1088, 1093,
1105, 1114, 1128, 1137, 1142, 1180, 1201, 1238, 1257, 1264, 1284, 1332,
1353, 1362, 1372, 1384, 1395, 1424, 1445, 1457, 1465, 1479, 1483, 1543,
2956, 2987, 2997, 3002, 3017, 3033, 3106, 3685, 3724, 3736, 3740, 3742

[a] Wavenumbers are not scaled.

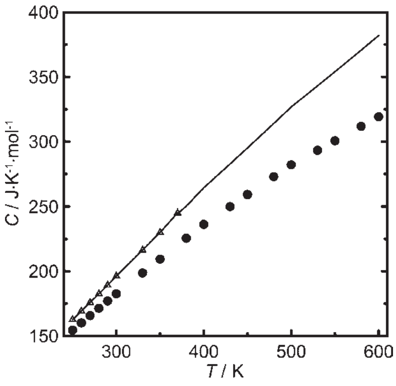

Figure 6. Correlation of isobaric heat capacity for microcrystalline cellulose (▲, smoothed values; −, calculated by eq 5) and vibrational contribution to heat capacity of glucose (●).

Our measurements did not confirm the heat capacity anomalies between (300 and 350) K reported in refs 7 and 8 and the concave heat capacity curves between 140 and 300 K observed in refs 5 and 6. The heat capacity of microcrystalline cellulose from this work and refs 3, 4, and 8 are compared in Figure 5. In the low-temperature region, the differences between the data from ref 8 and this work were not systematic. The substantial deviation was observed only above T = 270 K. Uryash et al.[8] assigned the discontinuity in the heat capacity curve between (280 and 290) K to the γ transition. However, the observed discontinuity can also be explained by the presence of water in the sample. The heat capacity change extrapolated to T = 273.15 K was 0.014 J·K^{-1}·g^{-1} which corresponded to w = 0.007 of water in the sample if one assumes water to have an additive contribution to the heat capacity of the sample.

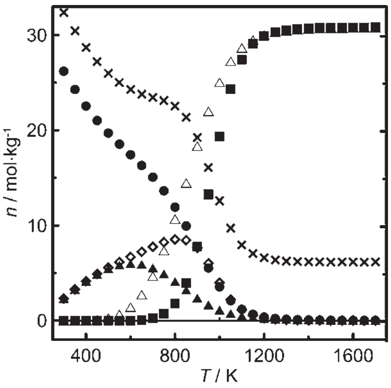

Figure 7. Equilibrium compositions for cellulose pyrolysis: ●, H_2O; ◇, CO_2; ▲, CH_4; ×, C; ■, CO; △, H_2. P = 1 bar, initial T = 300 K.

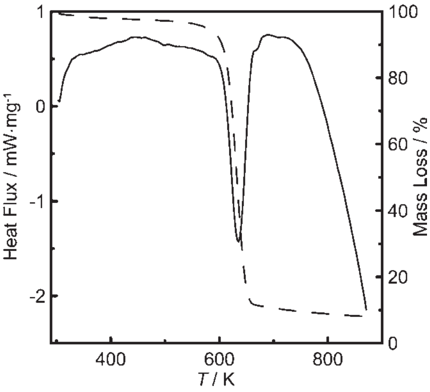

Figure 8. DSC (solid line) and TG (dashed line) curves for microcrystalline cellulose.

Table 6. Standard Molar Enthalpies of Combustion and Formation for Cellulose Samples

	$-\Delta_c U_m°$(298.15 K)	$-\Delta_c U_m°$(298.15 K)^a	$-\Delta_c H_m°$(298.15 K)^a	$-\Delta_f H_m°$(298.15 K)^a
sample	kJ·g^{-1}	kJ·g^{-1}	kJ·mol^{-1}	kJ·mol^{-1}
1	17.28 ± 0.04	17.29 ± 0.04	2803 ± 7	985 ± 7
2	16.61 ± 0.11	16.61 ± 0.11	2694 ± 17	1094 ± 17
3	17.43 ± 0.04	17.51 ± 0.04	2840 ± 7	949 ± 7
4	16.97 ± 0.05	16.98 ± 0.05	2748 ± 8	1040 ± 8

[a] For the ashfree sample.

The glass transition temperature of cellulose was observed at about (393 to 398) K.[3] If one assumes the T_g/T_{fus} quotient to be 0.7,[3] the expected temperature of fusion will be about 580 K. We extrapolated the heat capacity of microcrystalline cellulose to its estimated temperature of fusion using the equation similar to eq 2:

$$\frac{C_{p,\mathrm{m}}(\text{cellulose})}{C_{\mathrm{vib,m}}(\text{glucose})} = A + B(T/\mathrm{K}) \tag{5}$$

where $C_{p,\mathrm{m}}$ (cellulose) is the heat capacity of microcrystalline cellulose at temperature T and $C_{\mathrm{vib,m}}$(glucose) is the vibrational contribution to the heat capacity of glucose. The frequencies of normal vibrations of the glucose molecule (Table 5) were calculated for the most stable conformer at the B3LYP/6-31G(d) theory level using the Firefly software.[18,19]

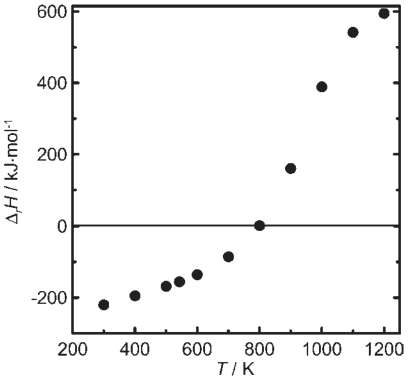

Figure 9. Temperature dependence of the enthalpy of the equilibrium cellulose thermolysis process.

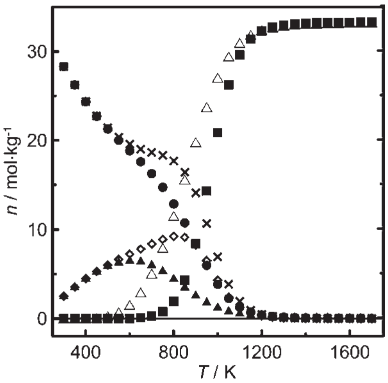

Figure 10. Equilibrium composition of reaction mixture for the initial composition (cellulose/H_2O = 1:1): ●, H_2O; ◇, CO_2; ▲, CH_4; ×, C; ■, CO; △, H_2. P = 1 bar, initial T = 300 K.

The vibrational contribution was calculated from the equation:

$$C_{\mathrm{vib,m}} = \sum_i R\left(\frac{h\nu_i}{kT}\right)^2 \exp\left(\frac{h\nu_i}{kT}\right)\left(\exp\left(\frac{h\nu_i}{kT}\right) - 1\right)^{-2} \tag{6}$$

where R is a gas constant, h is a Planck constant, k is a Boltzmann constant, and ν_i is a frequency of the ith normal vibration. The values of the coefficients $A = 0.9830$ and $B = 3.963 \cdot 10^{-4}$ for eq 5 were found by the method of least-squares from the experimental heat capacities of microcrystalline cellulose (1) and the vibrational contribution to the heat capacity of glucose in the temperature range (250 to 370) K. The results are presented in Figure 6.

Combustion Calorimetry. The energies of combustion determined in an isoperibol calorimeter are presented in Table 6. The enthalpies of formation of the cellulose samples were calculated based on the reaction

$$(C_6H_{10}O_5)_n(\mathrm{s}) + 6nO_2(\mathrm{g}) = 6nCO_2(\mathrm{g}) + 5nH_2O(\mathrm{l})$$

using $\Delta_f H_m^\circ(CO_2(g)) = -(393.15 \pm 0.13)$ kJ·mol^{-1} and $\Delta_f H_m^\circ(H_2O(l)) = -(285.83 \pm 0.04)$ kJ·mol^{-1}.[20] The energy of combustion for microcrystalline cellulose (1) calculated per gram of sample is in a very good agreement with that from ref 8 despite on possible unsufficient drying of the samples in the latter paper.

It was demonstrated in refs 8 and 21 that the enthalpies of combustion and formation of cellulose samples from the same origin linearly change with the degree of crystallinity. Microcrystalline cellulose is the most thermochemically stable form. According to our experiments, the differences in the energies of combustion for the studied samples reached 4 %, and this cannot be explained by the content of mineral components. The lower energy of combustion for amorphous cellulose compared to microcrystalline cellulose cannot be explained by different degrees of crystallinity. A possible explanation of the observed values is the difference in the degree of polymerization resulting from chemical treatment of the sample during preparation.

In the subsequent calculations, the value $\Delta_f H_m^\circ(298.15\ \mathrm{K}) = -(985 \pm 7)$ kJ per mole of monomeric units (Table 6) for the standard molar enthalpy of formation of microcrystalline cellulose was used.

Thermal Gasification of Cellulose. Thermocatalytic conversion of cellulose makes it possible to produce synthetic gas, which can be used both as gaseous fuel and inputs for various syntheses, as well as organic acids, levoglucosan, and hydrocarbons. In the processes of cellulose pyrolysis resulting in formation of

Table 7. Adiabatic Temperatures of Conversion and Equilibrium Compositions for $(C_6H_{10}O_5)_n$−H_2O−O_2 Mixtures at the Initial T = 300 K and P = 1 bar

initial amount/mol			content in equilibrium mixture[a]						T_a	$\Delta_c H_m^\circ$ [b]	$\Delta_c H_m^\circ$(gas) [c]
cellulose	H_2O	O_2	H_2O	CO_2	CH_4	C	CO	H_2	K	kJ·mol^{-1}	kJ·mol^{-1}
1			2.075	1.368	0.7334	3.710	0.189	1.459	775.6	−2455	−995
1	1		2.678	1.597	0.970	3.305	0.129	1.383	745.6	−2449	−1149
1	1	1	1.505	2.029	0.346	1.188	2.437	3.804	919.0	−2355	−1887
1		2	1.848	1.152	0.000	0.000	4.848	3.152	1474	−2134	−2134

[a] In mole per mole of cellulose monomeric units. [b] Lower heating value for the equilibrium mixture per mole of cellulose monomeric units. [c] Lower heating value for the gaseous components of the equilibrium mixture per mole of cellulose monomeric units.

synthetic gas, CH_4, $C_{(s)}$, CO_2 can also be formed in addition to CO and H_2.[22] Our results confirm that cellulose is thermodynamically unstable even at $T = 298.15$ K. Thermodynamic parameters of the reaction

$$(C_6H_{10}O_5)_n \rightarrow 6nC(s) + 5nH_2O(l)$$

calculated using the data from Table 3 and ref 22 are $\Delta_rH^o(298\ K) = -444.2 \pm 7.0$ kJ, $\Delta_rS^o(298\ K) = 203.2 \pm 0.9\ J\cdot K^{-1}$, and $\Delta_rG^o(298\ K) = -504.7 \pm 7.0$ kJ per mole of cellulose monomeric units. It means that this equilibrium is almost completely shifted to the right side of the equation.

We calculated the equilibrium compositions for the products of cellulose thermolysis over the temperature range (300 to 1700) K by the method of minimization of isobaric potential.[23] The results are strongly dependent on the list of components allowed in the reaction mixture. In the reported calculations the following components were allowed: graphite, H_2, CO, CO_2, $H_2O(g)$, and CH_4. The selected compounds are the major components of the high-temperature pyrolysis mixture.[22] The equilibrium compositions at various temperatures and pressures are presented in Figure 7 and Tables S5 to S7 of Supporting Information. A significant amount of unreacted carbon (up to $w = 0.079$ at $T = 1200$ K) remains in the equilibrium mixture at all temperatures. Above $T = 1200$ K and ambient pressure, the gas phase almost completely consists of CO and H_2.

The TGA and DSC curves for microcrystalline cellulose (1) demonstrated that the intense decomposition of cellulose started at about 600 K and reached its maximum at 633 K (Figure 8). After this peak, the sample mass was only about 10 % of the initial mass. The enthalpy of the process was found to be 61 kJ per mole of cellulose monomeric units.

According to our calculations, the following net equation

$$(C_6H_{10}O_5)_n = 3.89nC_{graphite} + 1.14nCO_2 + 0.01nCO + 0.97nCH_4 + 2.72nH_2O + 0.35nH_2$$

corresponds to the equilibrium cellulose thermolysis at $T = 633$ K. The enthalpy of the equilibrium process is $\Delta_rH(633\ K) = -119$ kJ per mole of cellulose monomeric units, and the expected mass of solid residue is 29 % of the initial mass (Table S5 of Supporting Information). The exothermicity of the equlilbrium process decreases with temperature (Figure 9); however, it becomes endothermal only above $T = 800$ K.

All of these facts confirm that the decomposition of cellulose in DSC was the nonequilibrium process. The endothermal peak in the DSC curve can probably be considered as the melting of cellulose coupled with its decomposition into less thermodynamically favorable gases than CO_2 and H_2O, for example, CO and H_2. The equilibrium was not established because the gases left the cell.

When 1 mole of water per 1 mole of cellulose monomeric units is added, the major components of the equilibrium mixture at $T > 1200$ K are CO and H_2 (Figure 10 and Table S7 of Supporting Information). The lower heating value of microcrystalline cellulose is $\Delta_cH_m°(298.15\ K) = -2585\ kJ\cdot mol^{-1}$ of monomeric units. The lower heating value of the mixture formed from 1 mole of cellulose monomeric units and 1 mole of water at $T = 1200$ K is $\Delta_cH^o{}_m(298.15\ K) = -3058\ kJ\cdot mol^{-1}$.

Since the adiabatic pyrolysis temperature for the equimolar mixture of cellulose and water is $T_a = 746$ K, additional energy is required to heat the products to $T = 1200$ K, and their equilibrium conversion can be evaluated using the cycle:

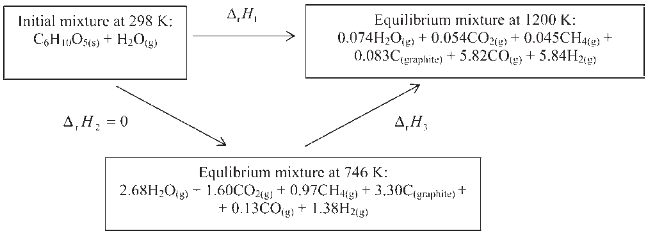

The reaction enthalpy Δ_rH_1 was determined from the cycle:

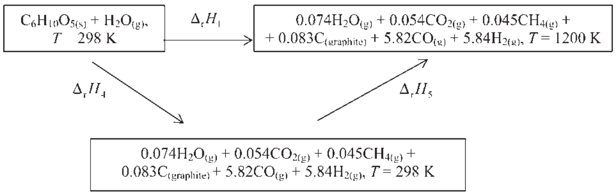

to be $\Delta_rH_1 = \Delta_rH_4 + \Delta_rH_5 = 541.3 + 330.5 = 871.8$ kJ per mole of cellulose monomeric units.

Therefore, the additional energy expenditure for obtaining the equilibrium mixture at $T = 1200$ K is $\Delta_rH_3 = \Delta_rH_1 = 871.8$ kJ per mole of cellulose monomeric units. So, the thermodynamically controlled conversion of cellulose resulting in formation of the equilibrium mixture at $T = 1200$ K leads to the 15 % loss of the lower energy value compared to the cellulose combustion. In technical realization of this process the energy consumed for heating of the initial mixture and the products can be returned using the high-grade heat flow ($0.074H_2O(g) + 0.054CO_2(g) + 0.045CH_4(g) + 5.82CO(g) + 5.84H_2(g)$). For example, the enthalpy change when mixture is cooled from (1200 to 400) K is $-295.2\ kJ\cdot mol^{-1}$, and only 4 % of the lower energy value is lost.

The temperature of 1200 K can be reached in the equilibrium adiabatic oxidative thermolysis because the adiabatic temperature of cellulose combustion in oxygen is very high: $T_a = 3026$ K. For the mixture $C_6H_{10}O_5/O_2 = 1{:}2$, the adiabatic reation temperature is 1474 K, and a mixture of gases with the lower heating value of -2134.4 kJ per mole of cellulose monomeric units (Table 7) is formed which is much less than the enthalpy of direct combustion of cellulose equal to $-2585.3\ kJ\cdot mol^{-1}$. It should be noted that the oxidative thermolysis of cellulose is normally realized with air as an oxidizer that results in decreasing adiabatic temperatures of conversion and specific (volumetric) energetic characteristics of burning gases.

■ ASSOCIATED CONTENT

Ⓢ Supporting Information. Experimental heat capacity and thermodynamic functions for cellulose samples 2, 3, and 4 (Table S1 to S4); equilibrium compositions of mixtures of cellulose pyrolysis and conversion with water (Tables S5, S6 and S7). This material is available free of charge via the Internet at http://pubs.acs.org.

■ AUTHOR INFORMATION

Corresponding Author

*Tel.: +375-17-2003916; e-mail: kabo@bsu.by.

Funding Sources

This work was financially supported by the Ministry of Education of the Republic of Belarus.

REFERENCES

(1) Sakovich, G. V.; Il'yasov, S. G.; Vasilishin, M. S.; Budaeva, V. V.; Egorov, V. U. The results of complex treatment of biomass. *Polzunovsk. Vestnik.* **2008**, *3*, 259–266.

(2) Mikhaylov, N. V.; Faynberg, E. Z. On the heat capacity and phase state of cellulose fibers of different structure. *Vysokomol. Soedin.* **1962**, *4*, 230–236.

(3) Faynberg, E. Z.; Mikhaylov, N. V. Investigation of the temperature dependence of heat capacity for cellulose fibers. *Vysokomol. Soedin.* **1967**, *9*, 920–926.

(4) Hatakeyama, T.; Nakamura, K.; Hatakeyama, H. Studies on heat capacity of cellulose and lignin by differential scanning calorimetry. *Polymer* **1982**, *23*, 1801–1804.

(5) Kozlov, N. A.; Rabinovich, I. B.; Medvedev, Z. N.; Sheyman, M. S.; Mochalov, A. N. Low-temperature heat capacity of cellulose from different methods of dehydration. *Khim. Tekhnol. Tsellul.* **1972**, *6*, 601–607.

(6) Karachevtsev, V. G.; Kozlov, N. A. Study of thermodynamic properties of cellulose at low temperatures. *Vysokomol. Soedin.* **1974**, *14*, 1892–1897.

(7) Uryash, V. F.; Rabinovich, I. B.; Mochalov, A. N.; Khlyustova, T. B. Thermal and calorimetric analysis of cellulose, its derivatives and their mixtures with plasticizers. *Thermochim. Acta* **1985**, *93*, 409–412.

(8) Uryash, V. F.; Larina, V. N.; Kokurina, N. U.; Novoselova, N. V. Thermochemical properties of cellulose and its mixtures with water. *Zh. Fiz. Khim.* **2010**, *84*, 1023–1029.

(9) Technical conditions 64-11-129-92. *Nutritional powdered microcrystalline cellulose "Ankir"(microcrystalline cellulose)*; Moscow, 1992.

(10) Shishonok, M. V.; Torgashov, V. I.; Gert, E. V.; Zubets, O. V.; Kaputski, F. N. Investigation of conditions for nitric acid delignification of rye straw. *Cellul. Chem. Technol.* **1997**, *31*, 425–438.

(11) Torgashov, V. I.; Shishonok, M. V.; Gert, E. V.; Kaputski, F. N. *Production of amorphous cellulose and its recrystallization in "mild" conditions through unstable derivatives*, Abstracts of All-Union Workshop "Methods of Cellulose Investigation", Riga, USSR, 1988; p 27.

(12) USSR Standard GOST 3877-88. *Petrochemicals. A Method of Sulfur Determination by Combustion in a Calorimetric Bomb*; Standards Publishing House: Moscow, 1989; pp 5−8.

(13) Segal, L.; Creely, J. J.; Martin, A. E.; Conrad, C. M. An Empirical Method for Estimating the Degree of Crystallinity of Native Cellulose Using the X-Ray Diffractometer. *Text. Res. J.* **1959**, *29*, 786–794.

(14) Pavese, F.; Malyshev, V. M. Routine measurements of specific heat capacity and thermal conductivity of high-T_c superconducting materials in the range 4−300 K using modular equipment. *Adv. Cryog. Eng.* **1994**, *40*, 119–124.

(15) Blokhin, A. V.; Kabo, G. J.; Paulechka, Y. U. Thermodynamic Properties of [C_6mim][NTf_2] in the Condensed State. *J. Chem. Eng. Data* **2006**, *51*, 1377–1388.

(16) Kabo, G. J.; Blokhin, A. V.; Kabo, A. G. Investigation of thermodynamic properties of organic substances. *Chemical Problems of Creation of New Materials and Technologies*; Ivashkevich, O. A., Ed.; BSU: Minsk, 2003; Vol. 1, pp 176−193.

(17) Kelley, K. K.; Parks, G. S.; Huffman, H. M. A new method for extrapolating specific heat curves of organic compounds below the temperature of liquid air. *J. Phys. Chem.* **1929**, *33*, 1802–1805.

(18) Granovsky, A. A. *Firefly*, version 7.1.G; MSU: Moscow, 2010.

(19) Schmidt, M. W.; Baldridge, K. K.; Boatz, J. A.; Elbert, S. T.; Gordon, M. S.; Jensen, J. H.; Koseki, S.; Matsunaga, N.; Nguyen, K. A.; Su, S.; Windus, T. L.; Dupuis, M.; Montgomery, J. A. General atomic and molecular electronic structure system. *J. Comput. Chem.* **1993**, *14*, 1347–1363.

(20) Chase, M. W. *NIST-JANAF Thermochemical Tables*, 4th ed.; National Institute of Standards and Technology: Gaithersburg, MD, 1998.

(21) Yelovich, M. Y. *Enthalpies of formation and dissolution of cellulose*, Proceeding of XII All-Union Conference on Chemical Thermodynamics and Calorimetry, Gor'kiy, USSR, 1988; pp 189−191.

(22) Kislov, V. M.; Glazov, S. V.; Chervonnaya, N. A.; Patronova, L. I.; Salganskaya, M. V.; Manelis, G. B. Gasification of biomass in a hyperadiabatic heating mode of combustion. *Khim. Tverd. Topl.* **2008**, *3*, 9–14.

(23) *Thermochemistry and Equilibria of Organic Compounds*; Frenkel, M., Ed.; VCH Publications: New York, 1993.